

Voice Recognition Robotic Dog Guides For Visually Impaired People

R.Rangarajan, Mrs.B.Benslija M.E.,

P.G.Scholar Dept. of Electronics & Communication Engg., Sri Muthukumaran Institute of Technology
Chennai, TamilNadu, India

Assistant Professor Dept. of Electronics & Communication Engg., Sri Muthukumaran Institute of Technology
Chennai, TamilNadu, India

Abstract: The primary purpose of this dog is to guide the visually impaired and elderly people to some predefined destination avoiding obstacles and traffic. It is also designed to act as an advanced multipurpose human assistance and service robot that is able to recognize the words spoken by the user, talk to them and take action according to the spoken voice command. Voice commands are recognized by an android smartphone and the information is transferred to the main MCU using a Bluetooth serial port that runs Bluetooth SPP protocol stack. The robotic dog has the ability to follow a human when commanded with voice. Touch sensitive e-skin senses human finger touch and helps answering complex user requests such as time, date and weather conditions such as light and temperature. The same can be asked using voice also. It even allows the user to set wake up alarm. A built in audio playback system can play music tracks in MP3 format. One of the music tracks is kept as the alarm tone. It also plays the role of a regular watchdog during night and barks like any normal dog if it finds any abnormal activity. During the day time it can charge itself by moving around within a given region in order to find the maximum sun light, intelligently avoiding the shaded areas, thereby freeing the user completely from maintenance issues such as battery charging.

I. Introduction

As many countries step into the aging society rapidly, more and more elders suffer from deficits of motor function or disability of the limbs, which are usually caused by neurological problems or lack of muscle strength. In addition, the growing elderly population causes the shortage of people for nursing care. Therefore, there is a great need to develop rehabilitation robots that can partially replace the nurses and the therapists. Currently, plentiful studies on rehabilitation robots can be found, including the applications for the upper limb, for the lower limb, and for the assisting or training of the whole body. In daily life, the walking is one of the most important human activities. To improve the walking ability of the elderly, the walker-type rehabilitation robot has become a popular research topic over the last decade. There have been many intelligent walker-type robots comprising active or passive wheels and supporting frame. A novel assistive robotic walker called "JAIST active robotic walker (JARoW)" to provide potential users with sufficient ambulatory capability in an efficient, cost-effective way. The Hitomi system to help the blind in outdoor environment was proposed already. The personal aid for mobility and monitoring (PAMM) system to provide mobility assistance and user health status monitoring was proposed already. A new intelligent walker based on passive robotics to assist the elderly, handicapped people, and the blind was proposed. There are still many deficiencies in the present walker systems. First, many walkers are designed for the indoor environment. Second, most of them are big in size and/or heavy in weight. An indoor robot is often restricted within limited places. Big size makes it impossible to be used in narrow space and heavy weight restricts the manoeuvrability. Many elders and patients are not so weak that they have to be nursed carefully. Nevertheless, sufficient support, such as a cane or stick, is necessary to help them take a walk outside, which enables them to realize high-quality lives or accelerate the rehabilitation. In these cases, an intelligent cane system may be more useful than walkers due to its flexibility and handiness. A Smart-Cane system is also proposed, which has a relative smaller size and nonholonomic constraint in kinematics. The nonholonomic constraint is useful for moving along a path stably, but reduces the manoeuvrability of the system. The "Guide Cane" and a robotic cane "Roji" are proposed for blind or visually impaired pedestrians to navigate safely and quickly through obstacles and other hazards. In the living environment, including the narrow space, the cane system is expected to be movable in Omni directions. Thus, omnidirectional mobile platform is needed in the robot design. This kind of platform has been considered in some applications, whereas their designs are special and not commercially available. Particularly, they are proposed for walker systems but cane systems, which are much smaller in size. Recently, commercial Omni wheels are applied in the area of walker systems. The problem that slender rollers of Omni wheels have limited load capacities is partly solved by the modern technology. In addition, a small omnidirectional platform can be constructed by this kind of wheels. In our previous study, an intelligent cane system was designed based on a

commercially available three-wheeled omnidirectional platform. We also investigated the fall detection and fall-prevention function of the cane robot systems. The recognition of user's walking intention plays an important role in the study of the walker-type rehabilitation robots. From the viewpoint of the control system of robot, the walking intention provides a real-time reference trajectory for the robot motion controller. Therefore, the more accurately the walking intention is inferred, the more satisfactory the control performance of the robot may be obtained. A manufacturing system that is controlled based on the human intention/desire was proposed. The dance partner robot, which estimates the intention of human dancer, was proposed. When we pay attention to the walker-type walking support system, similar researches can be found. In the study of motion-intention-recognizing approaches, the EMG-based methods are widely applied. However, the EMG signals are easily influenced by the location of electrodes, the thickness of fattiness, the body temperature, and the perspiration. Meanwhile, the information of the EMG signals is so large that a complicated pre-processing procedure is required before using them as the control input. In this paper, we improved our former intelligent cane system and studied its motion control problems in several situations based on estimating human walking intention. The human walking behaviour is described by switching walking modes. To model the human walking intention, an important concept called "intentional direction" (ITD) is proposed, as well as its dynamic model during human walking. Without knowing the ITD accurately, it is not an easy task to design a motion controller of the cane robot for an elderly or a handicapped user. Normally, these people cannot walk along their ITD clearly and smoothly due to their weak or handicapped lower limbs. For instance, even an elderly intends to walk straightforwardly, he/she might finally walk along a zigzag trajectory because of stumbling. Therefore, the interactive forces measured by the cane robot consist of plentiful user's unintentional walking information, which is part of the observation noise in the dynamic model of ITD. Comparing with a young healthy subject, apparently this observation noise of ITD is much bigger. Thus, it is necessary to pick up the ITD as accurately as possible from the noisy measurement. After that we may design a robot motion controller based on the ITD to aid the user's walking in accordance with his actual walking intention. Some filtering technologies are used to online estimate the ITD, based on which a new force control scheme called "intention-based admittance control (IBAC)" is proposed to provide a natural and intuitive interface for elderly users.

II. Omnidirectional-Type Robot

As stated in Section I, the aim of our intelligent cane robot is to perform optimized actions to help the user's walking or facilitate their recovery. These actions include "guiding," "fall preventing," "rehabilitation training," and so on. To provide these optimized actions, one of the most important tasks that should be accomplished by the robot is to correctly estimate the user's walking intention online. From the viewpoint of the robot control system, the user's walking intention provides a reference trajectory for the robot motion controller. Therefore, in this paper, we focus on the design of robot motion control strategy, in which the user's walking intention should be explicitly involved. This control strategy plays an important role in the design of a safe, reliable, and compliant cane robot, which is the prerequisite of the "rehabilitation training" for the elderly and disabled. In this section, we first introduce a prototype system of an omnidirectional-type cane robot shown in Fig. 2, which is developed to help the elderly walking and training their walking ability. The cane robot consists of an omnidirectional mobile base, a metal stick, and sensor groups including the force sensor, tilt angle sensors, and the laser range finders (LRFs). The omnidirectional mobile base comprises three commercially available omniwheels and actuators, which are specially designed for the walker systems. Despite the small size, the load capacity of this mobile base is up to 50 kg. A six-axis force/torque sensor is used as the main control input interface. The force sensor plays an important role in the estimation of human walking intention, which is illustrated in the following sections. Two LRFs are used to measure the distances between the stick and the knees and between the stick and the body, respectively. According to the online-acquired distance information, the fall-prevention function of the cane robot can be implemented as in [33]. We use two tilt angle sensors to measure the slope angle when the cane robot is located on a slope. This angle is useful in the calculation of gravity compensation. The current position and posture of cane robot are inferred from the sensory data of encoders mounted on the Omni wheels. To ensure the safety of cane robot, some measures are also taken. In the pre-processing of measured force signals, thresholds are used to get rid of outliers caused by impulsive external disturbances. The output of motion controller is also restricted by some thresholds, which can avoid the sudden change of robot movement. On the other hand, the state of user is monitored by multiple sensors. If any emergency state is detected, the robot is braked to avoid possible injury to the user.

III. Modeling And Estimation Of Human Walking Intention

ITD and Its State Model

In order to facilitate the development of dynamic model and control strategy, the coordinate systems of cane robot is illustrated first. As shown in Fig. 3(a), the coordinate system $O-x_0y_0z_0$ is the reference frame. The

coordinate system $O-x_1y_1z_1$ rotates with the slope angle α around the axis x_0 . The slope plane is denoted by Π . The local coordinate system is fixed on the cane robot and rotates with the yaw angle ψ . $O-x_r y_r z_r$ is the local coordinate system fixed on the cane robot. To describe the human walking intention during using the cane robot, an important concept is introduced as follows. *Definition 1:* The direction to which a person intends to move is referred to as the ITD. As shown in Fig. 4, the ITD can be evaluated by the angle between the forward direction (along with the axis y_r) and the ITD itself. Obviously, the ITD is a time-dependent value and is denoted by $\rho(n)$ in the rest of the paper. Furthermore, the quantity of this intention is characterized by the measured resultant force $F\rho(n)$ along the ITD. Note that discrete time scale n is assumed for the requirement of filtering technology. To formulate the walking intention quantitatively, it is required to obtain the dynamic model of ITD. The first thing we should do is to enumerate possible human walking modes. Although there are plentiful of possible modes during walking, only several of them are often used in the daily life. In this study, five simple walking modes are considered, which are listed in Table I. We assume that there are three main types of walking modes including “Stop” (mode I), “Go straight” (mode II), and “Turn around” (mode III) in daily life. Furthermore, mode II can be categorized into two submodes, “go straightforward” (mode IIa) and “go straight in other directions” (mode IIb). A typical case of human walking mode IIb is the fast lateral move to avoid a coming car. Mode III also can be further categorized into two submodes, “turn to the right” (mode IIIa) and “turn to the left” (mode IIIb). During walking, empirically, we know that transitions may occur between any two walking modes. Therefore, all possible transitions among the five modes are illustrated in Fig. 1. Empirically, we have following assumptions on the walking intention in different walking modes.

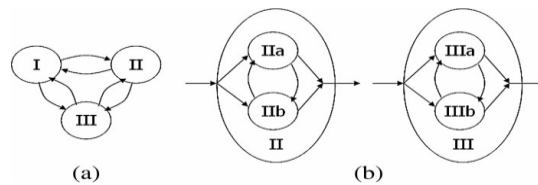


Fig. 1. Transition diagram of possible move modes

Assumption 1: In mode I, the ITD is supposed to be always zero.

Assumption 2: In mode II, the ITD is supposed to be a constant.

Assumption 3: In mode III, the ITD monotone converges to zero from an initial nonzero value.

Assumption 3 is proposed based on the natural behaviour when a person turns around. At the beginning of mode IIIa, normally there is a certain target to which one wants to move, which generates the initial ITD of the mode. During the process of turning around, the value of $\rho(n)$ gradually decreases and finally converges to zero, which causes a transition to mode I or II. In terms of the enumerated walking modes and given assumptions, a hybrid state model of ITD is described as

$$\rho(n + 1) = A\sigma(n) \cdot \rho(n), \sigma(n) \in \{I, II, III\} \quad (1)$$

where $\sigma(n)$ denotes the different walking mode given by Table I. The state transition matrices are given by

$$A_I = 0, A_{II} = 1, A_{III} = a(n) \quad (2)$$

where $a(n)$ satisfies $0 < a(n) < 1$.

Observation Model of ITD Based on the Human–Robot Interaction Force

Obviously, the ITD is indicated by the interaction force between the user and the cane robot. To compensate the gravity effect on the force sensor, first, we analyse the static forces exerted on the upper part of stick. P is used to denote the contact point between the force sensor and the upper part of stick. ${}^r\mathbf{F}$ and ${}^r\mathbf{n}$ are the force and torque exerted on the upper part of stick by the force sensor, respectively. ${}^r\mathbf{G}$ denotes the gravity force of the upper part of stick. ${}^r\mathbf{l}$ is the vector from point P to the centre of gravity of the upper part of stick. In the rest of paper, we use a superscript on the left side of a vector to indicate the coordinate frame in which the coordinate value is represented. To maintain the static equilibrium, the required force ${}^r\mathbf{F}^*$ and torque ${}^r\mathbf{n}^*$ are given by

$${}^r\mathbf{F}^* + {}^r\mathbf{G} = 0$$

and

$${}^r\mathbf{n}^* + {}^r\mathbf{l} \times {}^r\mathbf{G} = 0. \quad (4)$$

Let us assume

$${}^r\mathbf{F}^* = \begin{bmatrix} f_x^* \\ f_y^* \\ f_z^* \end{bmatrix} \quad \text{and} \quad {}^0\mathbf{G} = \begin{bmatrix} 0 \\ 0 \\ mg \end{bmatrix}. \quad (5)$$

From the two aforementioned equations, we have

$$\begin{bmatrix} f_x^* \\ f_y^* \\ f_z^* \end{bmatrix} = \begin{bmatrix} mg \cdot \sin \psi \sin \alpha \\ mg \cdot \cos \psi \sin \alpha \\ -mg \cdot \cos \alpha \end{bmatrix}. \quad (6)$$

During the walking procedure supported by the cane robot, let us suppose that the measured force and torque at time n satisfy

$${}^r\mathbf{F}(n) = [f_x(n) \quad f_y(n) \quad f_z(n)]^T$$

and

$${}^r\mathbf{n}(n) = [n_x(n) \quad n_y(n) \quad n_z(n)]^T. \quad (7)$$

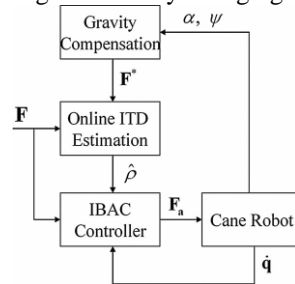
Then, the observation model of ITD can be described as

$$y(n) = \tan^{-1} \left(\frac{f_x(n) - f_x^*}{f_y(n) - f_y^*} \right) = \rho(n) + \omega(n) \quad (8)$$

where $\omega(n)$ is a combination of sensor noises and human gait habit. Note that the observation model is available for all the three modes. Everyone has a particular gait habit when walking. For example, some people will unintentionally move laterally when they walk straightforward. For simplicity, we assume $\omega(n)$ is a white noise sequence with a direction-dependent covariance $Q(\rho)$ that differs from person to person. For the same person, experiments show that $Q(\rho)$ is almost the same for different directions. This makes it possible to use traditional Kalman filter to estimate the ITD based on (1) and (8).

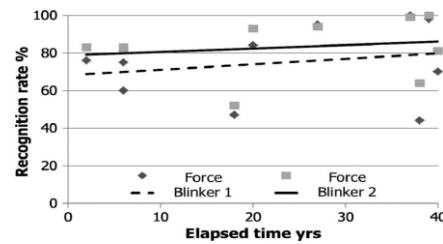
Motion Analysis

Next, we analysed the movement of the rotational weight. First, the rotational angle and velocity were measured using the encoder. Figs. 13 and 14 show the results of the control performance of the rotational angle and velocity, respectively. The average error between the reference angle and measured angle is 2.7 ± 3.0 (deg), while the maximum error is 11(deg). The maximum error occurred when the angular velocity was decreased by motor braking. This control performance is sufficient to indicate four directions (forward, backward, left, and right). Second, we confirmed the position of the weight from the viewpoint of the variable radius interface. The rotational movement was recorded from above using a high-speed camera (Keyence, VW-6000). The sampling frequency was 1000 (Hz). As shown, the weight moves by changing the rotational radius.



IV. Methodology

A subject in a sitting posture grasped the haptic interface “Force Blinker.” In this experiment, four directions (forward, backward, left, and right) were presented 80 times (20 trials were conducted for each direction). The traveling directions were randomly selected. Each subject tested the conditions of Force Blinker 2, with a variable distance between the weight and rotational axis, and those of the conventional method, Force Blinker 1, with a fixed distance between the weight and rotational axis, at the maximum rotational radius of Force Blinker 2. To avoid the habituation of feeling the direction with the haptic interface, the first condition was randomly selected. Ten visually impaired subjects, of whom eight are Class 1 (where the sum of visual acuity is less than 0.01) and two are Class 2 (where the sum of visual acuity is between 0.02 and 0.04), evaluated the developed system. A subject evaluating the fixed radius interface before the variable radius interface is defined as “Fix,” whereas a subject evaluating the variable radius interface before the fixed radius interface is defined as “Vari.” This experiment was approved by Waseda University IRB (#2009-142). The subjects received a detailed explanation of the experimental objectives and were told that they could stop the experiment at any time. We obtained each subject’s consent to the experimental conditions.



Relationship between recognition rate and elapsed time.

Experiment on the Flat Ground

In the experiments, for illustrating the validity of the IBAC control strategy, subject A utilized the cane robot to implement two series of walking modes. The inferred ITDs and their observations based on force signals are shown in Figs. 14(a) and 15(a). Trajectories of the estimated mode are also shown in these figures, where we use integers from 1 to 5 to denote the five walking modes sequentially (see the value of mode trajectory depicted by the dotted line). Note that even if there are some fault recognitions of mode transition, the performance of the rule-based mode transition function is sufficiently satisfactory in practice. In the experimental results, the main fault recognitions of mode transitions are mistaking mode IIa for mode IIb. This will not affect the system performance much because mode IIa is actually a special case of mode IIb. The advantage of fast detection of mode IIa is to quickly get an accurate ITD estimation, i.e., $\hat{\rho}(n) = 0$, which can be used to guide the motion control very clearly. However, even mode IIa is mistaken for mode IIb, the ITD that is estimated by the Kalman filter is nearly equal to zero and smooth enough to obtain a satisfactory intention-based motion control. As mentioned earlier, the Kalman filter and robust Kalman filter are used in modes II and III, respectively. Coefficient a in model (3) satisfies $a(n) = a_0 + \Delta a(n)$ with $a_0 = 0.93, |\Delta a(n)| < 0.3$. Comparing with the observation $y(k)$ from the noisy force signals, the online-estimated ITD $\hat{\rho}(n)$ reflects the human intention smoothly and distinctly, which provides explicit guidance to the IBAC controller. In particular, when the subject moves straightforward, which is the walking mode in most of the time, the inferred ITD is exactly the forward direction. This reduces meaningless lateral movements of the cane robot to a great extent. In addition, typical force responses are shown in Figs. 14(b) and 15(b) of the walking experiments.

Experiment on Slope

To further verify the proposed intention-based motion control strategy, some experiments were also performed on a slope with an angle of 5° . Subject A was asked to implement two series of walking modes with the aid of the cane robot. One experiment is to climb the slope, while turning to the right. The other experiment is to climb the slope straightforward and suddenly laterally move to the right (to pretend to avoid a coming obstacle). The experimental data of the user performing the first experiment. At the beginning and the end of the experiment, the recognized mode is "go straight." This is because the turning torque M_z is very small in these cases. Obviously, these fault recognitions will not affect the control performance much because any turning action is started and ended by a short "go straight" mode. The result of the second experiment is depicted. In this experiment, all the modes are recognized correctly. When the user went forward, the ITD was estimated as 0. When the user turned to the right, the estimated ITD is nearly equal to $\pi/2$. F_ρ and v_ρ are the measured force and velocity, which are along the ITD. F_v and v_v are the measured force and velocity, which are along the direction perpendicular to the ITD. Note that F_ρ and F_v are the effective forces in which the gravity effect has been eliminated. The robot velocity is 0 when F_ρ and F_v are zero, which demonstrates that the gravity compensation is effective. Velocity v_v is approximately 0 during the whole experiment, and it does not depend on the force F_v . Velocity v_ρ depends on the force F_ρ . These facts prove the effectiveness of our IBAC strategy in the experiments on the slope.

V. Results and Discussion

The recognition rates with the rotational radius either fixed in the conventional interface, Force Blinker 1, or variable to reduce the opposite presented force in the developed interface, Force Blinker 2. The data for subject #8 were eliminated, because he did not finish the experiment. The recognition rate of Force Blinker 1 was 74.9% (S.D. 20.1%) and that of Force Blinker 2 was 83.0% (S.D. 16.2%). The difference between the recognition rates of Force Blinker 1 and Force Blinker 2 was statistically significant ($p < 0.02, Z = -2.25$). For the statistical analysis, a Wilcoxon sign rank sum test, which is a nonparametric method, was used. We used this test because the number of acquired data was less than 50, the two groups were correlated, and the distribution of the parent population was not estimated as a Gaussian distribution. The recognition rate was improved by applying the variable radius mechanism in Force Blinker 2 instead of the fixed radius mechanism in Force Blinker 1. Second, we analysed the difference between the recognition rates of the different traveling directions. The recognition results for each direction are summarized in Table II. The recognition rate when the backward

direction was presented is higher than that when the right and left directions were presented ($p < 0.05$). Moreover, the relationship between the traveling direction and recognized direction was analysed when false recognition occurred. The false recognition rates as the direction was moved counter clockwise by 90° , 180° , and 270° to the traveling direction are 4%, 6%, and 6%, respectively. This shows that there is no direction for which it is easier to recognize a false direction.

Third, the relationship between the recognition rate and time from the onset of impaired sight was analysed. The relationship between recognition rate of Force Blinker 1 and 2 and the elapsed time of the disability. The approximated lines of Force Blinker 1 and 2 were calculated using the least squares method. It was confirmed that the value of the slope for both lines was positive. In other words, the longer the elapsed time is, the higher the recognition rate is. People who have had impaired sight for a long time are more sensitive to the presented force in the travelling direction. In addition, the approximated recognition rate of Force Blinker 2 is higher than that of Force Blinker 1 for all of the elapsed times. Finally, the validity of the recognition rate of the Force Blinker 2 was discussed. According to users who participated in this experiment, from the viewpoint of operability, one miss recognition is acceptable in a journey. Given that the maximum travelling distance is 1000 (m) with an intersection every 25 (m), the number of intersections is 40. Therefore, the required specification of the recognition rate is about 97% (= $39/40$). When subjects had difficulty accurately recognizing the presented direction in this experiment, the different directions were not felt absolutely. Therefore, accurate recognition may be improved by increasing the number of times the directions are presented, that is, the number of weight rotations. The required specification may be achieved by rotating the weight twice, because the apparent recognition rate, that is, the recognition percentage when the direction is presented twice, is $97.8\% (= 1 - (1 - 0.85) \times (1 - 0.85))$.

VI. Conclusion

In this paper, we developed a new haptic interface called "Force Blinker 2" for navigation by the visually impaired. In Force Blinker 2, a rotating weight and repulsive magnets are used to reduce the generated force in the opposite direction to the traveling direction by making the rotational radius variable depending on the velocity of the rotational weight. By changing from Force Blinker 1 to Force Blinker 2, the generated force in the opposite direction decreases by approximately 25%. It was confirmed using the encoder and a high-speed camera that the rotational weight is controlled by changing the rotational radius. Ten visually impaired subjects evaluated Force Blinker 2 by comparing it with Force Blinker 1, which is a fixed radius interface. The results show that the recognition rate of the traveling direction using Force Blinker 2 is approximately 85%, which is about 10% greater than that of Force Blinker 1. In both Force Blinker systems, people who have had impaired sight for a longer time were more sensitive to the traveling direction. In the future, we intend to integrate a route decision system with a cane containing the built-in haptic interface.

References

- [1] Y. Oonishi, S. Oh, and Y. Hori, "A new control method for power-assisted wheelchair based on the surface myoelectric signal," *IEEE Trans. Ind. Electron.*, vol. 57, no. 9, pp. 3191–3196, Sep. 2010.
- [2] [Online]. Available: <http://www.dbtk.mhlw.go.jp>
- [3] S. Shoval, I. Ulrich, and J. Borenstein, "NavBelt and the guide-cane [obstacle-avoidance systems for the blind and visually impaired]," *IEEE Robot. Autom. Mag.*, vol. 10, no. 1, pp. 9–20, Mar. 2003.
- [4] N. Takatori, K. Nojima, M. Matsumoto, K. Yanashima, and K. Magatani, "Development of voice navigation system for the visually impaired by using IC tags," in *Proc. 28th Annu. Int. Conf. IEEE Eng. Med. Biol. Soc.*, 2006, pp. 5181–5184.
- [5] T. O. Hoydal and J. A. Zelano, "An alternative mobility aid for the blind: The 'ultrasonic cane'," in *Proc. IEEE 17th Annu. Northeast Bioeng. Conf.*, 1991, pp. 158–159.
- [6] I. Shim and J. Yoon, "A robotic cane based on interactive technology," in *Proc. IEEE 28th Annu. Conf. Ind. Electron. Soc.*, 2002, vol. 3, pp. 2249–2254.
- [7] T. Tateishi, M. Murakami, M. Imura, Y. Yasumuro, T. Kuroda, Y. Mababe, and K. Chihara, "E-cane system with situation presumption for the blind," *Human Interface, Corresp. Human Interface*, vol. 4, no. 1, pp. 61–64, 2002.
- [8] S. Katsura and K. Ohnishi, "Human cooperative wheelchair for haptic interaction based on dual compliance control," *IEEE Trans. Ind. Electron.*, vol. 51, no. 1, pp. 221–228, Feb. 2004.
- [9] Y. Yokokura, S. Katsura, and K. Ohishi, "Stability analysis and experimental validation of a motion-copying system," *IEEE Trans. Ind. Electron.*, vol. 56, no. 10, pp. 3906–3913, Oct. 2009.
- [10] N. Ando, P. Korondi, and H. Hashimoto, "Networked telemanipulation systems "Haptic Loupe"," *IEEE Trans. Ind. Electron.*, vol. 51, no. 6, pp. 1259–1271, Dec. 2004.
- [11] S. Hyodo and K. Ohnishi, "A method for motion abstraction based on haptic information directionality and an application to haptic motion display system," *IEEE Trans. Ind. Electron.*, vol. 56, no. 5, pp. 1356–1363, May 2009.
- [12] H. Woo and D. Lee, "Exploitation of the impedance and characteristics of the human arm in the design of haptic interfaces," *IEEE Trans. Ind. Electron.*, vol. 58, no. 8, pp. 3221–3233, Aug. 2011.
- [13] H. Mori, R. Matsumoto, H. Kobayashi, and A. Mototune, "Prototype project on robotic travel aid," *J. Robot. Soc.*, vol. 19, no. 8, pp. 26–29, 2001.
- [14] S. Shoval, J. Borenstein, and Y. Koren, "Auditory guidance with the NavBelt—A computerized travel aid for the blind," *IEEE Trans. Syst., Man, Cybern. C, Appl. Rev.*, vol. 28, no. 3, pp. 459–467, Aug. 1998.
- [15] K. Tsukada and M. Yasumura, "Active belt: Belt-type wearable tactile display for directional navigation," in *Proc. Ubicomp*, 2004, pp. 384–399.

- [16] S. Sharmin, G. Evreinov, and R. Raisamo, "Non-visual feedback cues for pen computing," in *Proc. 1st Joint Eurohaptics Conf. Symp. Haptic Interfaces Virtual Environ. Teleoperator Syst.*, 2005, pp. 625–628.
- [17] S. Ertan, C. Lee, A. Willets, H. Tan, and A. Pentland, "A wearable haptic navigation guidance system," in *Proc. 2nd Int. Symp. Wearable Comput.*, 1998, pp. 164–165. ANDO *et al.*: HAPTIC INTERFACE "FORCE BLINKER 2" FOR NAVIGATION OF THE VISUALLY IMPAIRED 4119
- [18] L. Ran, S. Helal, and S. Moore, "An integrated indoor/outdoor blind navigation system and service," in *Proc. 2nd IEEE Int. Conf. Pervasive Comput. Commun.*, 2004, pp. 23-30.
- [19] T. Amemiya, H. Ando, and T. Maeda, "Phantom-DRAWN: Direction guidance using rapid and asymmetric acceleration weighted by nonlinearity of perception," in *Proc. Int. Conf. Augmented Tele-Existence Table Contents*, Christchurch, New Zealand, 2005, pp. 201–208.
- [20] T. Amemiya and T. Maeda, "Directional force sensation by asymmetric oscillation from a double layer slider-crank mechanism," *ASMEJ.Comput.Inf.Sci.Eng.*, vol.9,no.1,p011001,Mar.2009.
- [21] I. Ulrich and J. Borenstein, "The guidecane: Applying mobile robot technologies to assist the visually impaired," *IEEE Trans. Syst., Man, Cybern., A, Syst. Humans*, vol. 31, no. 2, pp. 131–136, Mar. 2001.
- [22] I. Shim, J. Yoon, and M. Yoh, "A human–robot interactive system RoJi," *Int. J. Control, Autom., Syst.*, vol. 2, no. 3, pp. 398–405, 2004.
- [23] H. Yu and S. Dubrowsky, "Omnidirectional mobility using active split offset castors," presented at the ASME IDETC/CIE 26th Biennial Mech. Robot. Conf., Sep. 10–13, 2006, Baltimore, MD.
- [24] Y. Hirata, T. Baba, and K. Kosuge, "Motion control of omnidirectionaltype walking support system "Walking Helper"," in *Proc. IEEEWorkshop Robot Human Interactive Commun.*, 2003, pp. 85–90.
- [25] L. Xie, Y. C. Soh, and C. E. de Souza, "Robust Kalman filtering for uncertain discrete-time systems," *IEEE Trans. Automat. Control*, vol. 39, no. 6, pp. 1310–1314, Jun. 1994.